Supporting Information

Bioconjugation of Hydroxylated Semiconductor Nanocrystals and Background-Free Biomolecule Detection

Yongwook Kim, Wonjung Kim, Hye-Joo Yoon, and Seung Koo Shin**

Bio-Nanotechnology Center, Department of Chemistry, Pohang University of Science and Technology, San 31 Hyojadong Namgu, Pohang, Kyungbuk 790-784, Korea

* To whom correspondence should be addressed. E-mail: hjyoon@postech.ac.kr, skshin@postech.ac.kr

Materials. Selenium powder (100 mesh, 99.99%), zinc acetate (99.99%), bis(trimethylsilyl) sulfide (synthesis grade), 1-octadecene (ODE, 90%), dodecylamine (98%), 3-mercapto-1-propanol (MPO, 95%), 3-mercaptopropionic acid (MPA, 99%), 4-morpholineethanesulfonic acid (MES, 99%) were purchased from Sigma-Aldrich.

Preparation of Organic-Soluble Nanocrystals. CdSe nanocrystals were prepared by reacting cadmium stearate with selenium powder in ODE at 210 °C (*1, 2*). Three monolayers of ZnS shells were epitaxially grown over the green-emitting CdSe core nanocrystals by reactions of zinc acetate with bis(trimethylsilyl) sulfide in ODE in the presence of dodecylamine at 150–200 °C. Resulting CdSe/ZnS nanocrystals were harvested, washed with methanol and acetone, and dried under vacuum (*2*).

Lattice Structure, Shape and Size Distribution of Nanocrystals. Powder X-ray diffraction (XRD) patterns of CdSe and CdSe/ZnS nanocrystals were taken with a Rigaku SWXD diffractometer. High-resolution transmission electron microscopy (HRTEM) images were obtained with JEOL JEM-2200FS HRTEM operating at 200 kV. HRTEM samples were prepared by placing a drop of a diluted chloroform solution containing nanocrystals on a 400-mesh copper grid from PELCO and wicking away liquid.

XRD patterns of CdSe core and CdSe/ZnS core/shell nanocrystals are shown in Figures S1a and b, respectively. Both the core and core/shell nanocrystals show the zinc-blende (ZB) lattice patterns, confirming epitaxial growth of the shell. HRTEM images of CdSe and CdSe/ZnS nanocrystals are shown in Figures S2a and b, respectively, and their size distributions are displayed in Figures S2c and d, respectively. CdSe core nanocrystals are nearly spherical in shape (2.4 ± 0.2 nm in diameter), and CdSe/ZnS nanocrystals are also spherical but larger in diameter (4.3 ± 0.4 nm).

Optical Characterization of Nanocrystals. Optical properties of nanocrystals are characterized, as previously described in detail (*3*). The absorption spectra were taken with an Agilent 8453 spectrophotometer. For the emission spectra and the PL decay measurement, nanocrystals were excited by 407 nm picosecond laser light (PicoQuant, LDH-P-C-405, 35 pJ per pulse laser). The emitted light was collected in backscattering geometry and fed into an optical fiber after filtering off the excitation light. The bifurcated optical fiber was connected to a spectrograph (Chromex, 250-IS, 300 gr mm^{-1}) equipped with a liquid-nitrogen (LN)-cooled charge-coupled device (CCD) (Princeton Instruments, LN/CCD-1024E) on one end to take the emission spectra and a monochromater (Acton Research, SP-150, 1200 gr mm^{-1}) equipped with a single-photon counting photon multiplier tube (PMT) (Becker & Hickl, PMC-100-1) on the other end to take PL decay. The PL decay was monitored with a single-photon counting PMT module (Becker & Hickl, SPC-630).

The band-edge absorption (λ_{abs}) occurs at 512 and 529 nm for organic-soluble CdSe and CdSe/ZnS nanocrystals in chloroform, respectively. The emission maxima (λ_{em}) appear at 524 and 549 nm for CdSe and CdSe/ZnS nanocrystals, respectively, with full width at half maximum (fwhm) of 28–30 nm.

The quantum efficiency (QE) increases from 5.3% of CdSe to 74% of CdSe/ZnS nanocrystals in chloroform. Optical properties (λ_{abs}, λ_{em}, fwhm, QE, and τ_{eff}) are listed in Table S1.

pH-Dependent Solubility of Water-Soluble Nanocrystals. CdSe/ZnS-MPO and CdSe/ZnS-MPA nanocrystals (10 pmol each) were added to three different buffer systems (100 μL each); propionate (pH 3.5–5.5), MES (pH 5.5–7.0), and PBS (pH 7.0–8.0). At each buffer system, pH was adjusted with either HCl (1 M) or NaOH (1 M). To check the pH-dependent solubility, we centrifuged the nanocrystal solution in each buffer for 1 min at 12,000 rpm. Fluorescent images were taken with a handheld UV (365 nm) lamp using a digital camera, as shown in Figure S3. CdSe/ZnS-MPO nanocrystals were not precipitated and remained soluble in the buffer in the entire pH range from 3.5 to 8.0, whereas CdSe/ZnS-MPA nanocrystals were precipitated below pH 5.0 but remained soluble above pH 5.5.

LITERATURE CITED

(1) Yang, Y. A., Wu, H., Williams, K. R., and Cao, Y. C. (2005) Synthesis of CdSe and CdTe nanocrystals without precursor injection. *Angew. Chem. Int. Ed. 44*, 6712–6715.

(2) Lim, S. J., Chon, B., Joo, T., and Shin, S. K. (2008) Synthesis and characterization of zinc-blende CdSe-based core/shell nanocrystals and their luminescence in water. *J. Phys. Chem. C 112*, 1744–1747.

(3) Kim, Y., Song, N. W., Yu, H., Moon, D. W., Lim, S. J., Kim, W., Yoon, H.-J., and Shin, S. K. (2009) Ligand-dependent blinking of zinc-blende CdSe/ZnS core/shell nanocrystals. *Phys. Chem. Chem. Phys. 11*, 3497–3502.

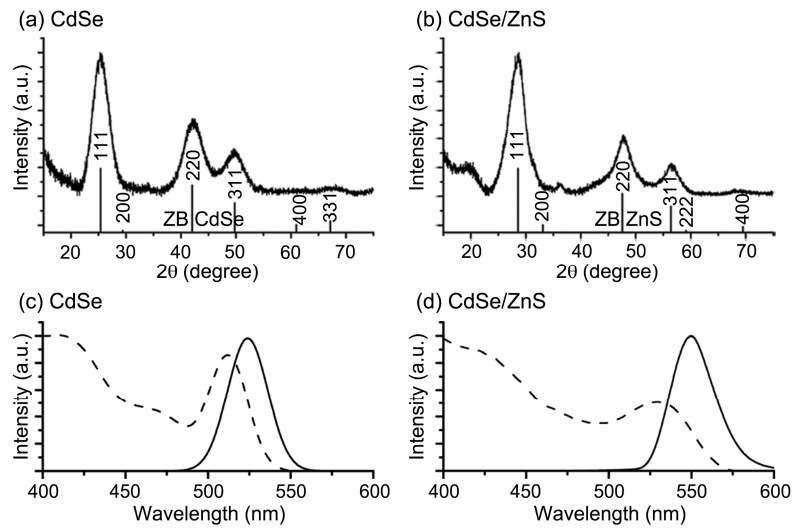

Figure S1. XRD patterns of (a) CdSe and (b) CdSe/ZnS nanocrystals. The vertical line represents the diffraction pattern of bulk zinc-blende lattice. Absorption (dashed line) and emission (solid line) spectra of (c) CdSe and (d) CdSe/ZnS nanocrystals.

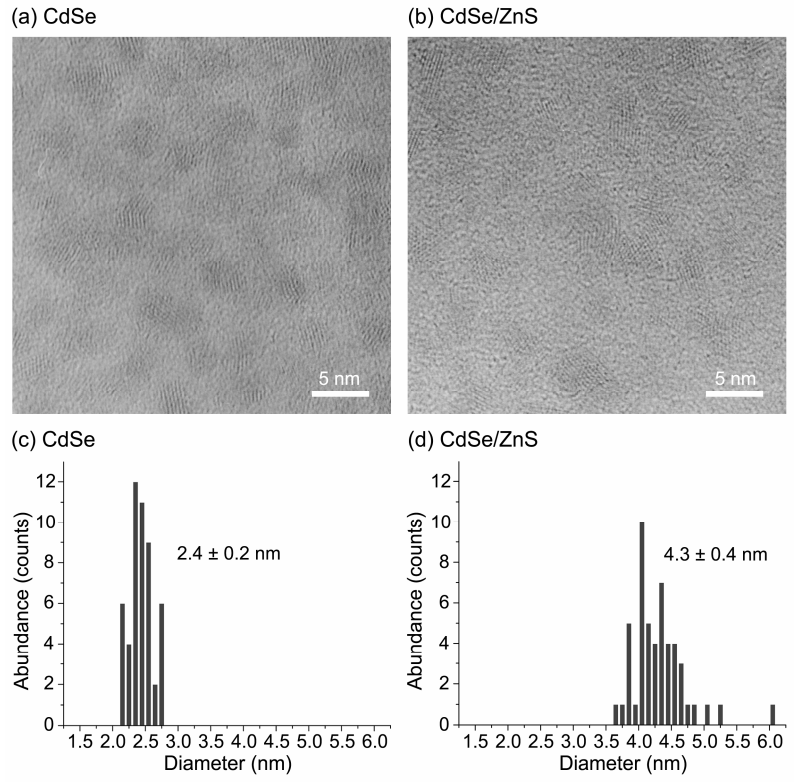

Figure S2. HRTEM images of (a) CdSe and (b) CdSe/ZnS nanocrystals and size distributions of (c) CdSe and (d) CdSe/ZnS nanocrystals. The average size is calculated from the distribution.

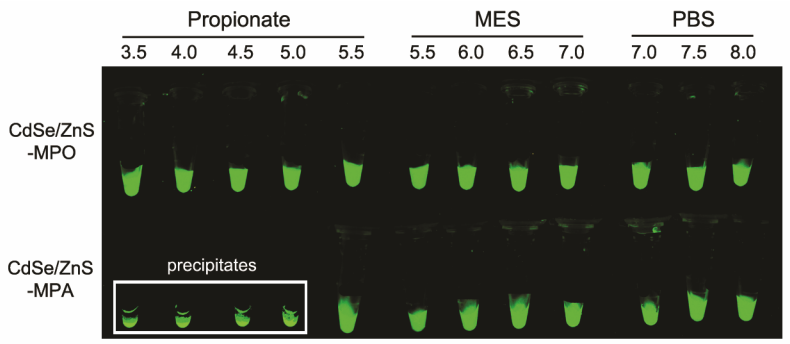

Figure S3. pH-dependent solubility of CdSe/ZnS-MPO (top) and CdSe/ZnS-MPA (bottom) nanocrystals in ten different pHs' between 3.5 and 8.0 using three buffer systems: propionate (pH 3.5–5.5), MES (pH 5.5–7.0), and PBS (pH 7.0–8.0).

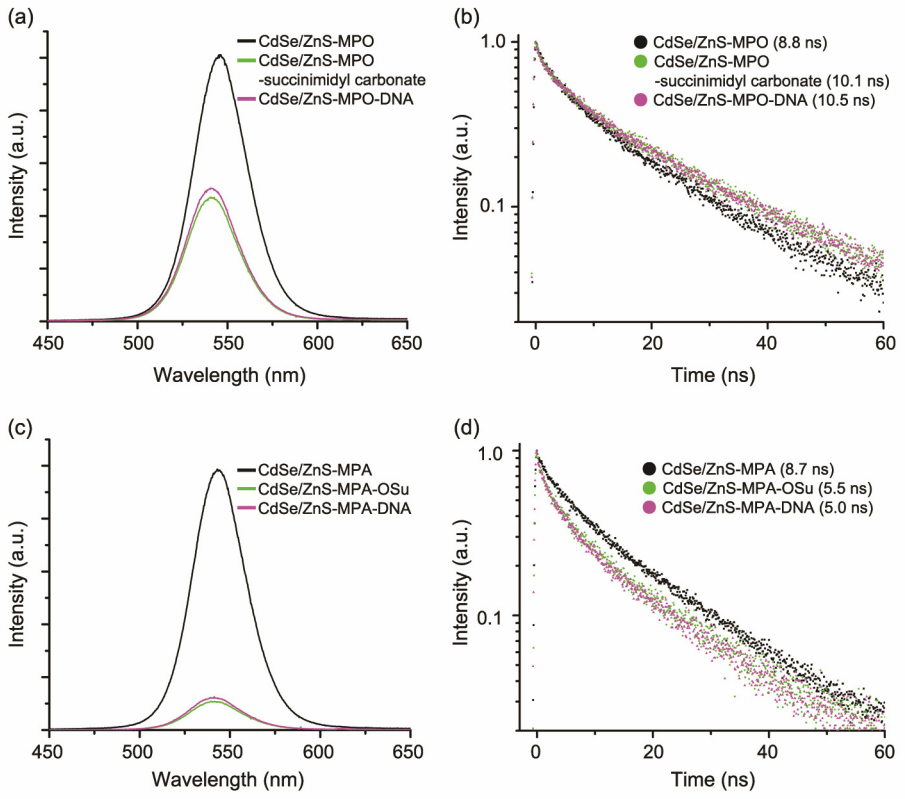

Figure S4. (a) Emission spectra and (b) PL decay of CdSe/ZnS-MPO nanocrystals (black), their succinimidyl carbonate derivatives (CdSe/ZnS-MPO-Su carbonate) (green), and nanocrystal-DNA-conjugates (magenta) in PBS; (c) emission spectra and (d) PL decay of CdSe/ZnS-MPA nanocrystals (black), their OSu esters (CdSe/ZnS-MPA-OSu) (green) and nanocrystal-DNA-conjugates (magenta) in PBS. λ_{em}, fwhm, and τ_{eff} are listed in Table S3.

Table S1. Optical Properties of CdSe and CdSe/ZnS Nanocrystals, Water-Soluble Nanocrystals, and Nanocrystal-Bioconjugates

sample	λ_{abs} (nm)	λ_{em} (nm)	fwhm (nm)	QE[d] (%)	τ_{eff}[e] (ns)
CdSe[a]	512	524	28	5.3	–
CdSe/ZnS[a]	529	549	30	74	16.9
CdSe/ZnS-MPO[b]	518	542	32	56	12.9
CdSe/ZnS-MPO-Biotin[c]	–	542	32	–	8.7
CdSe/ZnS-MPO-DNA[c]	–	542	32	–	9.0
CdSe/ZnS-MPO-HA[c]	–	542	32	–	8.4
CdSe/ZnS-MPA[b]	524	547	32	51	10.9
CdSe/ZnS-MPA-Biotin[c]	–	547	30	–	4.1
CdSe/ZnS-MPA-DNA[c]	–	547	30	–	3.7
CdSe/ZnS-MPA-HA[c]	–	547	30	–	4.1

[a] Organic-soluble nanocrystals in chloroform; [b] Water-soluble nanocrystals in water; [c] Nanocrystal-bioconjugates in PBS. HA: hemagglutinin; [d] Photoluminescence QE is relative to rhodamine 101 in ethanol (QE = 100%);
[e] Fitting parameters are listed in Table S2.

Table S2. Fitting Parameters for Photoluminescence Decay of Organic- and Water-Soluble Nanocrystals, and Nanocrystal-Bioconjugates

sample	τ_{eff}[d] (ns)	c_1	τ_1 (ns)	c_2	τ_2 (ns)	c_3	τ_3 (ns)
CdSe/ZnS[a]	16.9	0.07	0.58	0.14	5.2	0.79	20.4
CdSe/ZnS-MPO[b]	12.9	0.34	0.70	0.25	6.4	0.41	26.8
CdSe/ZnS-MPO-Biotin[c]	8.7	0.45	0.59	0.27	4.7	0.28	25.4
CdSe/ZnS-MPO-DNA[c]	9.0	0.46	0.50	0.26	5.0	0.28	26.6
CdSe/ZnS-MPO-HA[c]	8.4	0.46	0.53	0.28	5.0	0.27	25.2
CdSe/ZnS-MPA[b]	10.9	0.21	0.54	0.24	4.3	0.56	17.7
CdSe/ZnS-MPA-Biotin[c]	4.1	0.55	0.35	0.24	3.1	0.21	14.7
CdSe/ZnS-MPA-DNA[c]	3.7	0.58	0.56	0.24	3.5	0.17	14.4
CdSe/ZnS-MPA-HA[c]	4.1	0.56	0.42	0.26	3.7	0.19	15.6

[a] Organic-soluble nanocrystals in chloroform; [b] Water-soluble nanocrystals in water; [c] Nanocrystal-bioconjugates in PBS, HA: hemagglutinin; [d] $f(t) = c_1 \exp^{-t/\tau_1} + c_2 \exp^{-t/\tau_2} + c_3 \exp^{-t/\tau_3}$; $\tau_{eff} = c_1\tau_1 + c_2\tau_2 + c_3\tau_3$.

Table S3. Optical Properties of Water-Soluble Nanocrystals, Activated Nanocrystals, and Nanocrystal-DNA Conjugates in PBS

sample[a]	λ_{em} (nm)	fwhm (nm)	τ_{eff}[b] (ns)
CdSe/ZnS-MPO	545	34	8.8
CdSe/ZnS-MPO-succinimidyl carbonate	541	34	10.1
CdSe/ZnS-MPO-DNA	541	33	10.5
CdSe/ZnS-MPA	543	34	8.7
CdSe/ZnS-MPA-OSu	541	33	5.5
CdSe/ZnS-MPA-DNA	541	33	5.0

[a] Emission spectra and the PL decay of nanocrystals are shown in Figure S4; [b] Fitting parameters are listed in Table S4.

Table S4. Fitting Parameters for Photoluminescence Decay of Water-Soluble Nanocrystals, Activated Nanocrystals, and Nanocrystal-DNA Conjugates in PBS

sample	τ_{eff}[a] (ns)	c_1	τ_1 (ns)	c_2	τ_2 (ns)	c_3	τ_3 (ns)
CdSe/ZnS-MPO	8.8	0.34	0.41	0.31	4.6	0.36	20.4
CdSe/ZnS-MPO-succinimidyl carbonate	10.1	0.36	0.48	0.27	4.7	0.37	23.5
CdSe/ZnS-MPO-DNA	10.5	0.37	0.53	0.27	5.6	0.36	24.2
CdSe/ZnS-MPA	8.7	0.32	0.43	0.30	4.7	0.39	18.5
CdSe/ZnS-MPA-OSu	5.5	0.45	0.34	0.26	3.0	0.29	15.9
CdSe/ZnS-MPA-DNA	5.0	0.49	0.30	0.26	3.1	0.25	16.2

[a] $f(t) = c_1 \exp^{-t/\tau_1} + c_2 \exp^{-t/\tau_2} + c_3 \exp^{-t/\tau_3}$; $\tau_{eff} = c_1\tau_1 + c_2\tau_2 + c_3\tau_3$.